

Monaural Speech Enhancement with Recursive Learning in the Time Domain

Andong Li^{1,2}, Chengshi Zheng^{1,2}, Linjuan Cheng^{1,2}, Renhua Peng^{1,2}, Xiaodong Li^{1,2}

¹ Key Laboratory of Noise and Vibration Research, Institute of Acoustics, Chinese Academy of Sciences, Beijing, China

²University of Chinese Academy of Sciences, Beijing, China

{liandong, cszheng, chenglinjuan, pengrenhua, lxd}@mail.ioa.ac.cn

Abstract

In this paper, we propose a type of neural network with recursive learning in the time domain called RTNet for monaural speech enhancement, where the proposed network consists of three principal components. The first part is called stage recurrent neural network, which is proposed to effectively aggregate the deep feature dependencies across different stages with a memory mechanism and also remove the interference stage-by-stage. The second part is the convolutional auto-encoder. The third part consists of a series of concatenated gated linear units, which are capable of facilitating the information flow and gradually increasing the receptive fields. Recursive learning is adopted to significantly improve the parameter efficiency and therefore, the number of trainable parameters is effectively reduced without sacrificing its performance. The experiments are conducted on TIMIT corpus. Experimental results demonstrate that the proposed network achieves consistently better performance in both PESQ and STOI scores than two advanced time domain-based baselines in different conditions. The code is provided at <https://github.com/Andong-Li-speech/RTNet>.

Index Terms: noise reduction, recursive learning, time domain, convolutional network

1. Introduction

Speech is often degraded by background interference in real environments, which may significantly reduce the performance of automatic speech recognition (ASR), speech communication system and hearing aids. Monaural speech enhancement is dedicated to effectively extracting underlying target speech from its degraded version when only one channel of the noisy speech is available [1]. Existing signal-processing-based approaches include spectral subtraction [2], Wiener filtering [3] and statistical-based methods [4].

Recent advances in deep neural networks (DNNs) have facilitated the rapid development of speech enhancement research, and a great diversity of DNN models have been proposed to tackle the nonlinear mapping problem from the noisy speech to the clean speech (see [5, 6]). A typical DNN-based speech enhancement framework extracts temporal-frequency (T-F) features of the noisy speech and calculates some T-F representation targets of the clean speech. A model is then trained to establish the complicated mapping from the input features to the output targets with a supervised method. Training targets can be categorized into two types, where one is the masking-based [7] and the other one is the spectral mapping-based [6, 8].

Although the approaches based on the T-F domain are remarkable [6, 7, 8], they still have several limitations. Firstly, when the pre- and post-processing operations are applied using short-time Fourier transform (STFT) and inverse short-time

Fourier transform (iSTFT), the additional computational cost is inevitable. Specifically, STFT can be replaced by a type of one dimensional convolutional (1-D Conv) operation with fixed coefficients [9], and better performance is observed when they are adaptively learned from the training data. Secondly, conventional DNNs often estimate the magnitude of the spectrogram incorporated with the noisy phase to reconstruct the enhanced speech waveform, which restricts the upper performance and causes artifacts under low SNR conditions as phase continuity is important for speech perceptual quality [10]. Despite the fact that some networks based on phase recovery are proposed [11, 12], the results are still unsatisfactory. Moreover, the inconsistent problem will arise for most T-F domain-based networks [13, 14], i.e., no corresponding time-domain signal is guaranteed to exist for enhanced speech spectrogram.

Taking the above issues into account, a variety of time-domain-based networks have been proposed recently [15, 16, 17, 18]. Nonetheless, these processing systems often require a large number of trainable parameters, which may increase the computational complexity for practical applications. More recently, progressive learning (PL) has been applied in various tasks like single image deraining [19] and speech enhancement [20], where the whole mapping procedure is decomposed into multiple stages. In our preliminary work, we propose a progressive convolutional recurrent network (PL-CRN) [21], where the noise components are gradually attenuated with a lightweight convolutional recurrent network (CRN) in each stage. We attribute the success of PL to the accumulation of prior information with the increase of the stages, i.e., all the outputs in the previous stages actually serve as the prior information to facilitate the execution of subsequent stages. Motivated by this, we propose a novel time-domain-based network with a recursive mechanism called RTNet with much fewer trainable parameters. It works by recursively incorporating the estimated output from the last stage along with the original noisy feature back to the network, where each temporary output can be regarded as a type of state among different stages and thus trained with a recurrent approach. As a result, the feature dependencies across different stages can be fully exploited and the output estimation can be refined stage-by-stage.

The remainder of this paper is structured as follows. Section 2 formulates the problem and briefly introduces SRNN and GLU. The proposed architecture is described in Section 3. Section 4 presents the experimental settings. Experimental results and analysis are given in Section 5. Some conclusions are made in Section 6.

2. Network module

In the time domain, a mixture signal is usually formulated as $x(k) = s(k) + d(k)$, where k denotes the time index, $s(k)$, $d(k)$, and $x(k)$ are the clean speech, the noise, and the noisy

speech, respectively. The network aims to estimate the time-domain clean speech. The proposed architecture is in essence a type of multi-stage network, where the estimated output from the last stage combined with the original noisy input is sent back to the network. For notation convenience, we denote the frame vector of the noisy signal, estimation in l th stage, and the final output in the time domain as $\mathbf{x} \in \mathbb{R}^K$, $\tilde{\mathbf{s}}^l \in \mathbb{R}^K$, $\tilde{\mathbf{s}} \in \mathbb{R}^K$, respectively, where K is the frame length. The number of the stages is notated as Q . For the l th stage, the mapping process can be formulated as:

$$\tilde{\mathbf{s}}^l = g_\theta(\mathbf{x}, \tilde{\mathbf{s}}^{l-1}), \quad (1)$$

where $g_\theta(\cdot)$ represents the network function.

2.1. Stage recurrent neural network

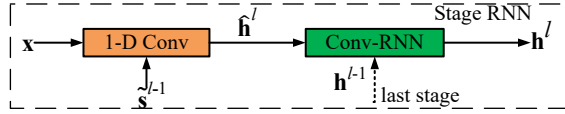


Figure 1: The internal detail of SRNN module. It includes a 1-D Conv block and a Conv-RNN block. The module is operated with double input and single output (DISO).

In this study, we explore the time dependencies of different stages and a type of recurrent convolutional structure named stage recurrent neural network (SRNN) is proposed. Theoretically, the learning process from the noisy feature to the clean target can be viewed as a type of sequence learning, where each state represents the intermediate output in one stage. As a consequence, the network can be trained following a recurrent learning paradigm. As shown in Fig. 1, SRNN contains two parts, namely 1-D Conv block and convolutional-RNN (Conv-RNN). Assuming the inputs are \mathbf{x} and $\tilde{\mathbf{s}}^{l-1}$, and the output of the 1-D Conv block is denoted as $\hat{\mathbf{h}}^l$. Then $\hat{\mathbf{h}}^l$ along with the hidden state vector from the last stage \mathbf{h}^{l-1} is sent to Conv-RNN to obtain a updated hidden state, i.e., \mathbf{h}^l . As a result, the inference of \mathbf{h}^l can be formulated as

$$\hat{\mathbf{h}}^l = f_{conv}(\mathbf{x}, \tilde{\mathbf{s}}^{l-1}), \quad (2)$$

$$\mathbf{h}^l = f_{conv_rnn}(\hat{\mathbf{h}}^l, \mathbf{h}^{l-1}), \quad (3)$$

where $f_{conv}(\cdot)$ and $f_{conv_rnn}(\cdot)$ represent the functions of 1-D Conv block and Conv-RNN block, respectively.

In this study, ConvGRU [22] is adopted as the unit for Conv-RNN, given as follows:

$$\mathbf{z}^l = \sigma(\mathbf{W}_z \circledast \hat{\mathbf{h}}^l + \mathbf{U}_z \circledast \mathbf{h}^{l-1}), \quad (4)$$

$$\mathbf{r}^l = \sigma(\mathbf{W}_r \circledast \hat{\mathbf{h}}^l + \mathbf{U}_r \circledast \mathbf{h}^{l-1}), \quad (5)$$

$$\mathbf{n}^l = \tanh(\mathbf{W}_n \circledast \hat{\mathbf{h}}^l + \mathbf{U}_n \circledast (\mathbf{r}^l \odot \mathbf{h}^{l-1})), \quad (6)$$

$$\mathbf{h}^l = (\mathbf{1} - \mathbf{z}^l) \odot \hat{\mathbf{h}}^l + \mathbf{z}^l \odot \mathbf{n}^l, \quad (7)$$

where $\sigma(\cdot)$ and $\tanh(\cdot)$, respectively, denote the sigmoid and the tanh activation functions. \mathbf{W} and \mathbf{U} refer to the weight matrixes of the cell. \circledast represents the convolutional operator and \odot is the element-wise multiplication. Note that all the biases are ignored for notation simplicity.

2.2. Gated linear unit

Gated convolutional layer is first introduced in [23] to model complicated interactions in the form of a gating mechanism which is beneficial to performance and its modified version

Table 1: Detailed parameter setup of the proposed architecture.

layer name	input size	hyperparameters	output size
convId_1	2×2048	(11, 2, 16)	16×1024
conv_rnn	16×1024	(11, 1, 16)	16×1024
convId_2	16×1024	(11, 1, 16)	16×1024
convId_3	16×1024	(11, 2, 32)	32×512
convId_4	32×512	(11, 2, 64)	64×256
convId_5	64×256	(11, 2, 128)	128×128
GLUs	128×128	$\begin{pmatrix} 1, 1, 64 \\ 11, 1, 64 \\ 1, 1, 128 \\ 1, 1, 64 \\ 11, 2, 64 \\ 1, 1, 128 \\ 1, 1, 64 \\ 11, 4, 64 \\ 1, 1, 128 \\ 1, 1, 64 \\ 11, 8, 64 \\ 1, 1, 128 \\ 1, 1, 64 \\ 11, 16, 64 \\ 1, 1, 128 \\ 1, 1, 64 \\ 11, 32, 64 \\ 1, 1, 128 \end{pmatrix}$	128×128
skip_1	128×128	-	256×128
deconvId_1	256×128	(11, 2, 64)	64×256
skip_2	64×256	-	128×256
deconvId_2	128×256	(11, 2, 32)	32×512
skip_3	32×512	-	64×512
deconvId_3	64×512	(11, 2, 16)	16×1024
skip_4	16×1024	-	32×1024
deconvId_4	32×1024	(11, 2, 1)	1×2048

named GLU is utilized in [24] by replacing the tanh nonlinearity with a linear unit and residual learning is also incorporated to mitigate gradient vanishing problem when learning deep features [25]. As shown in Fig. 2-(b), two additional branches are introduced compared with the conventional CNN block, where one is the gated operation controlled with sigmoid function to adjust the information flow percentage and the other is residual connection. Dilated convolution is applied to increase the receptive field, which is beneficial to capture sequence correlations among neighboring points. We use parametric ReLU (PReLU) [26] as the activation function and the kernel size is set to 11 herein.

3. Proposed architecture

The architecture of RTNet is illustrated in Fig. 2-(a), which includes three parts, namely SRNN, convolutional auto-encoder (CAE) [27] and a series of GLUs. SRNN consists of a 1-D Conv block and a ConvRNN block. 1-D Conv takes the concatenation of both noisy speech vector and the output estimation vector from the last stage along the channel axis. Therefore, the size of network input is $(2, K)$, where 2 refers to channels. After SRNN, the output is sent to the subsequent modules. CAE consists of the convolutional encoder and the decoder. The encoder consists of four 1-D Conv blocks, which compresses and establishes the deep representation of the features by halving the feature length with strided operation while consecutively doubling the channels. The decoder is the symmetric representation compared with the encoder, where the length of the feature is successively expanded through a number of deconvolutional layers [28]. Both encoder and decoder adopt PReLU as the activation nonlinearity except the output layer, where tanh is used to normalize the value range into $[-1, 1]$. Additionally, skip connections are adopted to connect each encoding layer to its homologous decoding layer, which compensates for the feature loss during the encoding process. To model the time correlations, six concatenated GLUs are inserted between the encoder and decoder, where the dilated rates are $(1, 2, 4, 8, 16, 32)$.

When the estimation output of the l th stage is obtained, i.e., $\tilde{\mathbf{s}}^l$, it is fed back and concatenated with the noisy input \mathbf{x} along

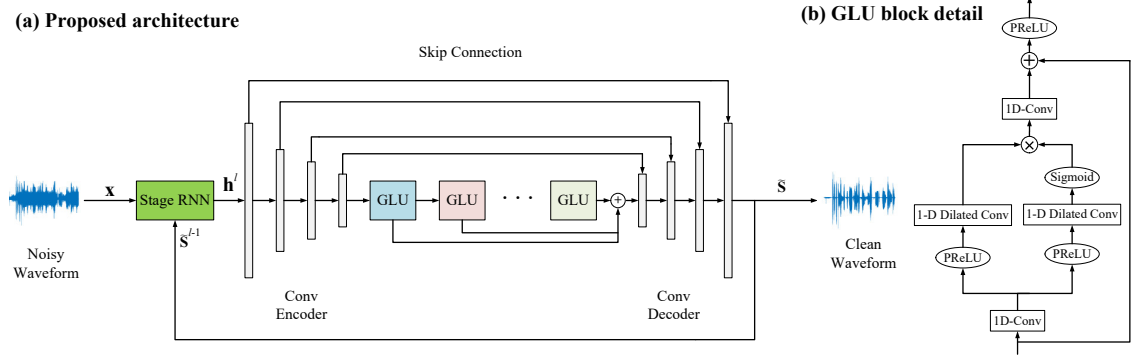


Figure 2: The framework of the proposed network RTNet with recursive learning. (a) The overview of RTNet. x , \tilde{s}^{l-1} , \tilde{h}^l and \tilde{s} denote the input feature, the estimation output in stage $l - 1$, the state in stage l and the final estimation output, respectively. (b) The detail of GLU adopted in this study, where PReLU is adopted and the kernel size is set to 11.

channel axis to execute the next recursive stage. Here we only impose supervision on the final output \tilde{s} , which is consistent with the setting in [19].

A more detailed parameter configuration of the proposed network is summarized in Table 1, where the input and output sizes of 2-D tensor representation are specified with $(Channels \times Framesize)$ format. The hyperparameters of the layers except GLUs are specified with $(KernelSize, Strided, Channels)$ format. The hyperparameters of GLUs are specified with $(KernelSize, DilatedRate, Channels)$ format. Bold numbers refer to the dilated rate.

4. Experiments

4.1. Datasets

Experiments are conducted on TIMIT corpus [29], which includes 630 speakers of eight major dialects of American English with each reading ten utterances. 1000, 200 and 100 clean utterances are randomly selected for training, validation and testing, respectively. Training and validation dataset are mixed under different SNR levels ranging from -5dB to 10dB with the interval 1dB while the testing datasets are mixed under (-5dB, -2dB) conditions. 130 types of noises (including 115 types used in [21], 9 types from [30], 3 types from NOISEX92 [31] and 3 common environmental noise, i.e. aircraft, bus and cafeteria) are used for training and validation. Another 5 types of noises from NOISEX92 (babble, f16, factory2, m109 and white) are used to explore the network generalization capacity.

Various noises are first concatenated into a long vector. During each mixed process, the cutting point is randomly generated, which is subsequently mixed with a clean utterance under one SNR condition. As a result, totally 10,000, 2000 and 400 noisy-clean utterance pairs are created for training, validation, and testing, respectively.

4.2. Baselines

In this study, two advanced time-domain-based networks are selected as the baselines, namely AECNN [17] and RHR-Net [18]. AECNN is a typical 1-D Conv-based auto-encoder architecture with a large number of trainable parameters. The number of channels in consecutive layers are $\{64, 64, 64, 128, 128, 128, 256, 256, 256, 512, 512, 256, 256, 128, 128, 128, 1\}$, with 11 and PReLU being the filter size and activation nonlinearity, respectively. RHR-Net has also the form

Table 2: Experimental results under seen noise conditions for PESQ and STOI. **BOLD** indicates the best result for each case. The number of stages Q are set to 3, 4 and 5 for model comparisons.

Metrics	PESQ			STOI (in %)			
	SNR	-5dB	-2dB	Avg.	-5dB	-2dB	Avg.
Noisy	1.47	1.66	1.57	63.03	68.20	65.62	
AECNN	2.25	2.49	2.37	82.70	87.51	85.11	
RHR-Net	2.32	2.55	2.44	83.13	87.90	85.51	
RTNet (Q = 3)	2.36	2.59	2.48	83.18	87.92	85.55	
RTNet (Q = 4)	2.35	2.59	2.47	83.75	88.39	86.07	
RTNet (Q = 5)	2.37	2.60	2.48	84.03	88.54	86.28	

Table 3: Experimental results under unseen noise conditions for PESQ and STOI. **BOLD** indicates the best result for each case. The number of stages Q are set to 3, 4 and 5 for model comparisons.

Metrics	PESQ			STOI (in %)			
	SNR	-5dB	-2dB	Avg.	-5dB	-2dB	Avg.
Noisy	1.44	1.67	1.56	59.64	67.45	63.55	
AECNN	1.88	2.20	2.04	77.37	85.10	81.24	
RHR-Net	2.06	2.35	2.21	78.13	85.82	81.98	
RTNet (Q = 3)	2.10	2.37	2.23	78.59	85.68	82.13	
RTNet (Q = 4)	2.06	2.35	2.21	79.31	86.20	82.76	
RTNet (Q = 5)	2.09	2.35	2.22	79.48	86.54	83.01	

of auto-encoder framework except all the convolutional layers are replaced by bidirectional GRU (BiGRU). In addition, direct skip connections are replaced by PReLU-based residual connections. It achieves state-of-the-art metric performance among several advanced speech enhancement models with limited trainable parameters (see [18]). The number of units per layer are $\{1, 32, 64, 128, 256, 128, 64, 32, 1\}$ and three residual skip connections are introduced. Note that the last layer is a single-directional GRU to produce the enhanced signal.

4.3. Experimental settings

We sample all the utterances at 16kHz. Each frame has a size of 2048 samples (128 ms) with 256 samples (16 ms) offset between adjacent frames. All the models are trained with mean absolute error (MAE) criterion, optimized by Adam algorithm [32]. The learning rate is initialized at 0.0002. We halve the learning rate only if consecutive three validation loss incre-

ment arises and the training process is early-stopped only if ten validation loss increment happens. We train all the models for 50 epochs. Within each epoch, the minibatch is set to 2 at the utterance level, where all the utterances are randomly chunked to 4 seconds if they exceed 4 seconds and zero-padded on the contrary.

5. Results and analysis

We evaluate the performance of different models in terms of perceptual evaluation of speech quality (PESQ) [33] and short-time objective intelligibility (STOI) [34].

5.1. Objective results comparison

The objective results are presented in Tables 2 and 3. One can observe the following phenomena. Firstly, all the models significantly improve the scores in terms of PESQ and STOI for both seen and unseen cases, whilst the proposed RTNet achieves the best performance among the three models. For example, for seen cases, when $Q = 3$, RTNet improves PESQ by 0.11 and 0.04, and improves STOI by 0.44% and 0.04% over AECNN and RHR-Net, respectively. This is because the memory mechanism is utilized to refine the network with a stage-wise manner and improve the parameter efficiency. A similar tendency is also observed for unseen cases. Secondly, when comparing between two baselines, RHR-Net obtains consistently better performance than AECNN, we argue that BiGRU is adopted as the basic component for both encoding and decoding process, which facilitates better temporal capture capability for long sequences than 1-D Conv, whose performance is limited by kernel size and dilation rate. This can also partly explain the limited advantages of RTNet over RHR-Net.

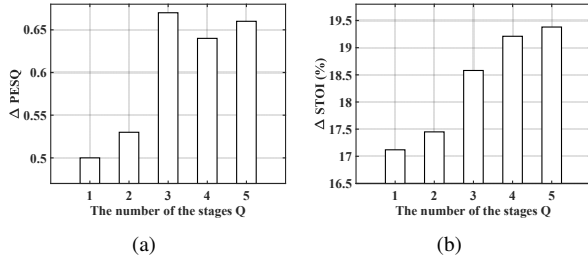


Figure 3: PESQ and STOI improvements with the increase of the number of the stages Q . The values are averaged over unseen dataset. Here five values are explored, i.e., $Q = 1, 2, 3, 4, 5$.

5.2. The influence of stage number Q

In this study, we explore the influence of the number of the stages Q , and it takes the values from 1 to 5. The metric improvements are given in Fig. 3. One can observe the following phenomena. Firstly, when $Q \leq 3$, both PESQ and STOI scores are consistently improved with the increase of Q , indicating that both metrics can be effectively refined with recursive learning. Nonetheless, when Q takes from 3 to 5, PESQ falls into saturation even slightly attenuation while STOI is further improved. This is because MAE is adopted as the loss criterion, whose optimization target is inconsistent with the objective evaluation criterion and can not further refine both metrics at the same time [35]. This phenomenon reveals that further optimization of MAE can facilitate the STOI but slightly suppress the further optimization of PESQ.

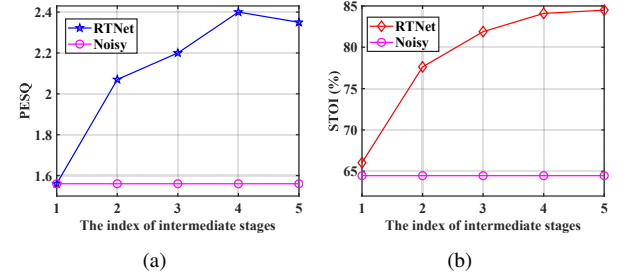


Figure 4: The metric scores in terms of PESQ and STOI for different intermediate stages given $Q = 5$. The results are averaged over both seen and unseen conditions. Noisy scores are also presented for comparison.

5.3. The insights on recursive learning

To analyze the advantages of recursive learning, we evaluate the metric scores of different intermediate stages when $Q = 5$ and the results are given in Fig. 4. As the figure shows, when the first recursive stage is finished, the estimation has similar metric scores over the noisy input. However, when the network is recursed for more stages, a notable improvement is observed. This can be explained as the increase of iteration will lead to the accumulation of prior information and it effectively complements the speech details of the current estimation. In addition, as SRNN is formulated with a memory mechanism, it is capable of selectively reserving useful information and dropping irrelevant interference. As a result, the network can better learn how to recover the speech information.

Table 4: The number of trainable parameters among different models. The unit is million. **BOLD** indicates the lowest trainable parameters.

Model	AECNN	RHR-Net	RTNet
Para. (million)	6.31	1.95	1.02

5.4. Trainable parameters and ideal network depth

The number of trainable parameters for the baselines and proposed RTNet is presented in Table 4. As the table shows, compared with AECNN and RHR-Net, RTNet further decreases the number of trainable parameters, which demonstrates the high parameter efficiency of recursive learning.

In order to improve network performance, a deeper network is needed, which usually results in more trainable parameters. With recursive learning, the network is reused for multiple stages, and we can explore a deeper network without any additional parameters. In this paper, considering the gradient flow, the number of the ideal layers for RTNet is $28 \times Q$, where 28 represents the number of layers for the feedforward gradient flow. Therefore, a deeper network can be explored by recursing the network for more stages.

6. Conclusions

In this study, we propose a type of recursive network in the time domain named RTNet for monaural speech enhancement. Stage RNN is proposed to effectively aggregate the deep features across different stages. In addition, concatenated GLUs are adopted to increase the receptive field while controlling the information flow. Experimental results demonstrate that RTNet achieves consistently better performance than the other two advanced time-domain baselines and effectively decreases the number of trainable parameters at the same time.

7. References

- [1] P. C. Loizou, *Speech enhancement: theory and practice*. CRC press, 2013.
- [2] S. Boll, "Suppression of acoustic noise in speech using spectral subtraction," *IEEE Transactions on acoustics, speech, and signal processing*, vol. 27, no. 2, pp. 113–120, 1979.
- [3] X. Hu, S. Wang, C. Zheng, and X. Li, "A cepstrum-based pre-processing and postprocessing for speech enhancement in adverse environments," *Applied acoustics*, vol. 74, no. 12, pp. 1458–1462, 2013.
- [4] S. H. Jensen, P. C. Hansen, S. D. Hansen, and J. A. Sorensen, "Reduction of broad-band noise in speech by truncated QSVD," *IEEE Transactions on Speech and Audio Processing*, vol. 3, no. 6, pp. 439–448, 1995.
- [5] D. L. Wang and J. Chen, "Supervised speech separation based on deep learning: An overview," *IEEE/ACM Transactions on Audio, Speech, and Language Processing*, vol. 26, no. 10, pp. 1702–1726, 2018.
- [6] Y. Xu, J. Du, L.-R. Dai, and C.-H. Lee, "A regression approach to speech enhancement based on deep neural networks," *IEEE/ACM Transactions on Audio, Speech and Language Processing (TASLP)*, vol. 23, no. 1, pp. 7–19, 2015.
- [7] Y. Wang, A. Narayanan, and D. Wang, "On training targets for supervised speech separation," *IEEE/ACM transactions on audio, speech, and language processing*, vol. 22, no. 12, pp. 1849–1858, 2014.
- [8] K. Tan and D. Wang, "A convolutional recurrent neural network for real-time speech enhancement," in *Interspeech*, 2018, pp. 3229–3233.
- [9] S. Venkataramani, J. Casebeer, and P. Smaragdis, "Adaptive front-ends for end-to-end source separation," in *Proc. NIPS*, 2017.
- [10] K. Paliwal, K. Wójcicki, and B. Shannon, "The importance of phase in speech enhancement," *speech communication*, vol. 53, no. 4, pp. 465–494, 2011.
- [11] D. S. Williamson, Y. Wang, and D. L. Wang, "Complex ratio masking for monaural speech separation," *IEEE/ACM Transactions on Audio, Speech and Language Processing (TASLP)*, vol. 24, no. 3, pp. 483–492, 2016.
- [12] S. W. Fu, T. Y. Hu, Y. Tsao, and X. Lu, "Complex spectrogram enhancement by convolutional neural network with multi-metrics learning," in *2017 IEEE 27th International Workshop on Machine Learning for Signal Processing (MLSP)*. IEEE, 2017, pp. 1–6.
- [13] J. Le Roux, N. Ono, and S. Sagayama, "Explicit consistency constraints for stft spectrograms and their application to phase reconstruction," in *SAPA@ INTERSPEECH*, 2008, pp. 23–28.
- [14] D. Griffin and J. Lim, "Signal estimation from modified short-time fourier transform," *IEEE Transactions on Acoustics, Speech, and Signal Processing*, vol. 32, no. 2, pp. 236–243, 1984.
- [15] S. Pascual, A. Bonafonte, and J. Serra, "SEGAN: Speech enhancement generative adversarial network," *arXiv preprint arXiv:1703.09452*, 2017.
- [16] D. Rethage, J. Pons, and X. Serra, "A wavenet for speech denoising," in *2018 IEEE International Conference on Acoustics, Speech and Signal Processing (ICASSP)*. IEEE, 2018, pp. 5069–5073.
- [17] A. Pandey and D. L. Wang, "A new framework for cnn-based speech enhancement in the time domain," *IEEE/ACM Transactions on Audio, Speech and Language Processing (TASLP)*, vol. 27, no. 7, pp. 1179–1188, 2019.
- [18] J. Abdulbaqi, Y. Gu, and I. Marsic, "RHR-Net: A residual hour-glass recurrent neural network for speech enhancement," *arXiv preprint arXiv:1904.07294*, 2019.
- [19] D. Ren, W. Zuo, Q. Hu, P. Zhu, and D. Meng, "Progressive image deraining networks: a better and simpler baseline," in *Proceedings of the IEEE Conference on Computer Vision and Pattern Recognition*, 2019, pp. 3937–3946.
- [20] T. Gao, J. Du, L.-R. Dai, and C.-H. Lee, "Densely connected progressive learning for lstm-based speech enhancement," in *2018 IEEE International Conference on Acoustics, Speech and Signal Processing (ICASSP)*. IEEE, 2018, pp. 5054–5058.
- [21] A. Li, C. Zheng, and X. Li, "Convolutional recurrent neural network based progressive learning for monaural speech enhancement," *arXiv*, vol. abs/1908.10768, 2019.
- [22] N. Ballas, L. Yao, C. Pal, and A. Courville, "Delving deeper into convolutional networks for learning video representations," *arXiv preprint arXiv:1511.06432*, 2015.
- [23] A. Van den Oord, N. Kalchbrenner, L. Espeholt, O. Vinyals, A. Graves *et al.*, "Conditional image generation with pixelcnn decoders," in *Advances in neural information processing systems*, 2016, pp. 4790–4798.
- [24] K. Tan, J. Chen, and D. L. Wang, "Gated residual networks with dilated convolutions for monaural speech enhancement," *IEEE/ACM Transactions on Audio, Speech, and Language Processing*, vol. 27, no. 1, pp. 189–198, 2018.
- [25] Y. N. Dauphin, A. Fan, M. Auli, and D. Grangier, "Language modeling with gated convolutional networks," in *Proceedings of the 34th International Conference on Machine Learning-Volume 70*. JMLR.org, 2017, pp. 933–941.
- [26] K. He, X. Zhang, S. Ren, and J. Sun, "Delving deep into rectifiers: Surpassing human-level performance on Imagenet classification," in *Proceedings of the IEEE international conference on computer vision*, 2015, pp. 1026–1034.
- [27] V. Badrinarayanan, A. Handa, and R. Cipolla, "Segnet: A deep convolutional encoder-decoder architecture for robust semantic pixel-wise labelling," *arXiv preprint arXiv:1505.07293*, 2015.
- [28] H. Noh, S. Hong, and B. Han, "Learning deconvolution network for semantic segmentation," in *Proceedings of the IEEE international conference on computer vision*, 2015, pp. 1520–1528.
- [29] J. S. Garofolo, L. F. Lamel, W. M. Fisher, J. G. Fiscus, and D. S. Pallett, "DARPA TIMIT acoustic-phonetic continuous speech corpus cd-rom. mist speech disc 1-1.1," *NASA STI/Recon technical report n*, vol. 93, 1993.
- [30] Z. Duan, G. J. Mysore, and P. Smaragdis, "Speech enhancement by online non-negative spectrogram decomposition in nonstationary noise environments," in *Thirteenth Annual Conference of the International Speech Communication Association*, 2012.
- [31] A. Varga and H. J. Steeneken, "Assessment for automatic speech recognition: II. NOISEX-92: A database and an experiment to study the effect of additive noise on speech recognition systems," *Speech communication*, vol. 12, no. 3, pp. 247–251, 1993.
- [32] D. P. Kingma and J. Ba, "Adam: A method for stochastic optimization," *arXiv preprint arXiv:1412.6980*, 2014.
- [33] A. W. Rix, J. G. Beerends, M. P. Hollier, and A. P. Hekstra, "Perceptual evaluation of speech quality (PESQ)-a new method for speech quality assessment of telephone networks and codecs," in *2001 IEEE International Conference on Acoustics, Speech, and Signal Processing. Proceedings (Cat. No. 01CH37221)*, vol. 2. IEEE, 2001, pp. 749–752.
- [34] C. H. Taal, R. C. Hendriks, R. Heusdens, and J. Jensen, "An algorithm for intelligibility prediction of time-frequency weighted noisy speech," *IEEE Transactions on Audio, Speech, and Language Processing*, vol. 19, no. 7, pp. 2125–2136, 2011.
- [35] S.-W. Fu, T.-W. Wang, Y. Tsao, X. Lu, and H. Kawai, "End-to-end waveform utterance enhancement for direct evaluation metrics optimization by fully convolutional neural networks," *IEEE/ACM Transactions on Audio, Speech, and Language Processing*, vol. 26, no. 9, pp. 1570–1584, 2018.